

# ROTOR DESIGN FOR AN UNMANNED HELICOPTER FOR USE ON MARS

Timothy W. Streett

Advisor: Dr. James F. Marchman

Virginia Polytechnic Institute

## **Abstract**

This project is a detailed investigation on rotors in rarefied atmosphere. It focuses on an analytical determination of the optimum configuration to lift a 100 kg payload effectively in Martian atmosphere. A simplified actuator disc model was used to get a ballpark power requirement to determine the overall feasibility of the concept. A more detailed blade element analysis will be used to determine the overall capability of the system.

Using highly idealized equations as a starting point for velocities at selected control points, more detailed analyses determine the theoretical capabilities of various selected airfoil designs for each rotor configuration. Airfoils will be selected based on published performance characteristics. The design constraints for size will be taken from the dimensions of the current Martian lander aero shells. The aerodynamic design will focus on keeping the tip-speed subsonic to avoid shock problems.

After the single rotor is defined, it will be examined in a co-axial configuration to show the benefits of that design choice over other options.

## **I. Justification for Research:**

Aircraft capable of flying in Martian atmosphere have been justified repeatedly, for purposes ranging from oblique mapping, obtaining better topographic detail than satellites can provide, to the precise delivery of small autonomous science pods that conduct on-site research. The most prevalent designs are descent deployed platforms similar to conventional airplanes or flying wings. There are numerous advantages to these designs, but there are several major flaws as well.

The first problem in the use of such fixed wing airplanes is mission duration. These craft deploy in the atmosphere, fly a simple descent, and crash. They cannot land safely and take off again without prepared surfaces, which are non-existent on Mars. Each aircraft flies a few hours, more or less, and cover one descent corridor. A vertical takeoff craft would be better able to cover a wide area, and with a renewable power source, be re-useable as long as the fuel cell holds out.

The second issue with fixed wing craft is one of controls. An automated flight program, as would be necessary with the long communication times between the vehicle and any earth based controller, would have more difficulty navigating a fixed wing craft in tight spaces. If some Martian

canyons or dense rock formations warranted study, forcing the craft to be in constant motion would require a much faster and more sophisticated AI. A vertical takeoff craft would have the ability to stop and analyze the situation before moving on, reducing crash probabilities with simpler AI routines.

One solution is the use of some form of rotary wing aircraft. A helicopter of moderate size would be capable of the mid-low altitude mapping that the conventional aircraft are currently being developed for, with the added benefit of wider mapping capabilities. A helicopter or similar craft would also allow for low stress ground deployment, which would lighten the structure of the vehicle itself, though this does require landing apparatus on the descent pod itself. Another benefit would be the ability to carry samples back to an on site automated lab or sample return rocket, while vastly out-ranging a land based rover. Its ability to land repeatedly would allow for imaging on the quality of the land rovers while maintaining the mapping capabilities of other aircraft.

## **II. The Design Problem:**

The question at hand is: Can a rotor be configured to function sufficiently well in the Martian environment to provide lift for a craft that can replace the functionality of the land based rovers? To that end, the design requirement was stated as followed:

“Design a rotor that can lift a 100 kg mass and fold to fit inside the same launch module as the Mars rovers with a maximum of one fold per blade.”

This statement was made assuming that 100 kg was sufficient to contain the structure, propulsion system, flight systems, and imaging equipment, as well as some payload capacity for sample return missions. This was left as an assumption, as the full design of a functional vehicle is somewhat beyond the scope of a one man undergraduate project. The fold limit on the blade was made to limit the size and complexity of the system. Theoretically, an infinitely long rotor would provide a very low disc loading and an easy takeoff, but is hardly practical to fold into a 3 meter space.

The first part of this investigation was to acquire a working understanding of both the atmosphere of Mars and the basics of helicopter flight. To that end, extensive reading of previously published papers on Mars flight was conducted, as well as many referenced articles on low Reynolds number flight, the performance regime that is most prevalent in such an environment.

The next step in the process was the determination of which, if any currently extant airfoils

would perform in the Mars atmosphere. The bulk of the search was through the University of Illinois at Urbana-Champaign airfoil database compiled by Michael Selig. This database of over 1500 airfoils contains representatives of the major NACA airfoil types, as well as a vast array of other airfoils from other parties. Many of them were independently tested, and the listing of files was deemed sufficient as a cross section of available airfoils.

The final step involved determining which airfoil would fulfill the requirements of performance at various station lengths along the blade of a rotor. To this end, the base-line performance parameters were calculated using an actuator disc approach. Final determination of configuration was done with a combined blade-element momentum theory. The rotor was designed only for hovering and vertical climb performance, as the forward flight problem was also far too complex. Also, the rotor should be optimized for hover, as the system is more likely to spend the majority of its time either hovering or landing/launching vertically.

### III. Atmospheric Conditions

Several studies of the atmosphere on Mars have been done in the past, both theoretical ideal atmospheric models and actual data collected by previous landers. The chemical composition is hostile, to say the least:

95.3% carbon dioxide (CO <sub>2</sub> ),
2.7% nitrogen (N <sub>2</sub> ),
1.6% argon (Ar),

**Table 1: Mars Atmospheric Conditions<sup>1</sup>**

There are also trace amounts of oxygen and water vapor, which are statistically insignificant. This has some effect on the aerodynamic properties, but the primary limit is on the type of propulsion systems that can be used. Whatever system is used must carry both fuel and oxidizer, if it is to be an “air breathing” engine, or be electrical. Since the idea is to have a highly re-usable craft, electrical engines seem to be most suitable, as they will run as long as the battery can be re-charged, via solar panels or some other method.

The physical properties of the Martian atmosphere are no more forgiving. The density, mean temperature, and pressure are all much lower than standard on earth. At Mars datum height, the reference constants are:

	Mars	Earth
<b>T [C]</b>	-31	15
<b>p [kPa]</b>	0.699	101.325
<b>Density [kg/m<sup>3</sup>]</b>	0.01503	1.225
<b>Speed of Sound [m/s]</b>	247.2059	340.29
<b>Viscosity [kg/m-s]</b>	1.228e-05	1.789e-05

**Table 2: Mars Datum Reference Conditions compared to Earth Sea Level<sup>2,3</sup>**

The harshest condition is the density. The density is two orders of magnitude lower than Earth sea level density. Since the aerodynamic forces involved in aircraft flight are governed in large measure by density, this loss is enormously significant, as will be discussed later.

$$a = \sqrt{gRT} \quad (1)$$

The gas constant for Mars is 192.1 J/kg·K, and the ratio of specific heats,  $\gamma$  is 1.289.<sup>3</sup> These, combined with the lower ambient temperature, results in the much lower speed of sound, per equation 1.

$$m = 0.0148 \left( \frac{402.69825}{0.555T + 240} \right) \left( \frac{T}{293.15} \right)^{\frac{3}{2}} * 0.001 \quad (2)$$

Equation (2) is Southerland’s relation for CO<sub>2</sub>, to find the viscosity in kg/ms. Since the Martian atmosphere is over 95% CO<sub>2</sub>, this is a sufficiently good approximation.

$$T = T_{datum} - 0.000998h \quad (3)$$

$$P = P_{datum} e^{-0.00009*h} \quad (4)$$

$$r = \frac{T}{PR} \quad (5)$$

Equations (3)-(5) are used to calculate the lapse behavior of the Martian atmosphere up to 7000m, which is more than enough for the operation of a low altitude observation aircraft. In the above, h is the height above datum in meters. These equations were used to compile a standard atmosphere table for Mars, included in appendix 1.<sup>3</sup>

The Martian atmosphere creates many difficulties for aircraft designers. These include the sonic and compressible behavior of the local air, the massively lower aerodynamic forces due to reduced density, and the Reynolds number based parameters like flow regime and airflow separation.

The compressibility effects caused by the low speed of sound have a large influence on useable velocities. Helicopters especially suffer from difficulty in sonic flow. If the rotor tip speed is to be supersonic, there are many more design constraints that must be adhered to

than for a subsonic rotor. The uneven shock stresses on the individual blades pose structural difficulties. In forward flight, unbalanced super/sub sonic behavior across the rotor disc also creates imbalances that must be addressed. To avoid these complications, the design was limited to a subsonic tip speed, which would have fewer risks of damage due to aerodynamic stresses. To keep all of the airflow over the tip subsonic, this limits the tip speed to 160~170 m/s depending on the acceleration due to the airfoil shape. This is a fairly normal tip speed for a medium sized rotor, and so is not too big of a concern, though it is the primary design point.

Aerodynamic constants are almost universally defined as a function of the dynamic pressure:  $\frac{1}{2}\rho V^2$ . With the densities being on the order of one hundredth of the densities typically dealt with on earth, the forces are reduced by the same margin. This, combined with the velocity limits discussed previously requires that the characteristic lengths/areas must be much larger to generate even a significant fraction of the lift an equivalent system would provide on Earth.

The biggest problem the low density environment causes is a severe reduction in the Reynolds number, defined:

$$Re = \frac{\rho VL}{\mu} \quad (6)$$

The low velocity and low density combine to bring the Reynolds number down between two and three orders of magnitude from the typical flight Reynolds numbers on Earth. If the each blade was half a meter wide, rather large for rotors, the tip Reynolds number would only be ~100,000, and it would grow progressively lower towards the hub. The problem this creates is with the flow over the airfoil. On most airfoils, at some point the flow will transition to a turbulent flow regime, which is necessary in ensuring the airflow stays attached all the way to the trailing edge in the face of the adverse pressure gradient on the back side. On a flat plate, the overall transition Reynold's number is ~250,000. Even in a high turbulence environment, the transition Reynolds number only drops to ~150,000. This is still slightly above what can be achieved over a cambered airfoil at the very tip of the rotor blade.

One possible solution would be to deliberately trip the flow at some point before separation, either by roughening the surface or placing wire trips on the airfoil, to force transition to turbulent flow. This, however, brings up the other big problem in low Reynold's number environments, flow hysteresis. In extremely low Reynolds number environments, a small laminar separation bubble

usually forms, right around the point on the wing where the pressure gradient becomes unfavorable. This is also the point at which the flow would need to be tripped. In tripping the flow, there is a risk of causing the laminar separation bubble at the front to expand, near instantaneously, and joining the normal separation region near the end of the airfoil. This produces a sudden stall, with all the associated negative effects, this is the start of a process called hysteresis. The serious difficulty with the hysteresis effect is that the angle of attack has to be reduced to a point much lower than the angle of attack at which the hysteresis effect started. Such a reduction is very difficult to achieve on a rotor without significant detrimental impact on the flight performance of the whole system. This effect is also realized near the maximum lift angle of attack, where it more closely simulates a sudden stall effect.<sup>4</sup>

The one advantage to trying to fly on Mars is the relatively lower gravity. Martian gravitational acceleration is only ~ 38% of Earth gravity, at 3.69 m/s. This makes up for at least some of the loss in available lift from the lower density, and makes flight possible.

#### **IV. Choosing the Airfoils:**

The atmospheric considerations above led to certain criteria for choosing an airfoil to use in the rotors. The first, most obvious requirement is functionality at low Reynold's number. Most traditional airfoils require a transition to turbulent flow to maintain flow attachment, which is difficult or impossible in the conditions spelled out above. To avoid stall hysteresis, the airfoils will have to work at well below their max  $C_L$ , meaning they need to be relatively high lift, even at very low angles of attack. Airfoils were selected from the Selig Database<sup>5</sup> based on those two criteria.

Since the traditional boundary layer analyses for drag are based on high Reynolds flow, any use of these methods is suspect. While methods like the Walz and Moses integral methods should still provide good information, their accuracy is greatly reduced. To avoid this problem, the search was restricted to a subset of the Selig database that had experimental data on the lift and drag. This still left over 600 airfoils, which was more than sufficient. The requirement was set that the airfoils have a  $C_L$  of at least 1 at an angle of attack of 7 degrees.

Based on the above criteria, two airfoils were selected. The two airfoils are the GM15 and MA409 airfoil. Both airfoils were classes as free flight flapper airfoils. They were the only two tested airfoils that met the requirement at Reynolds numbers between 30000 and 100000. The profiles are given below:

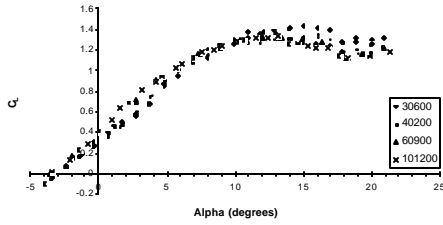


Figure 1: GM 15 Lift Curve at Various Re

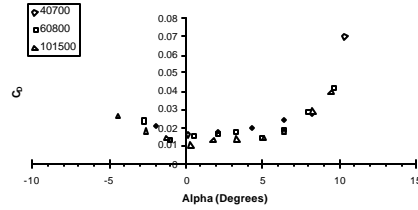


Figure 6: MA409 Drag Curves

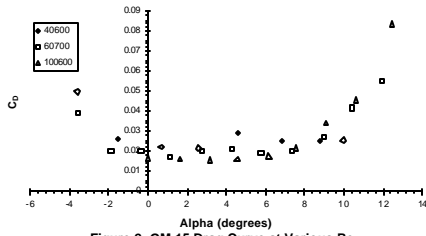


Figure 2: GM 15 Drag Curve at Various Re

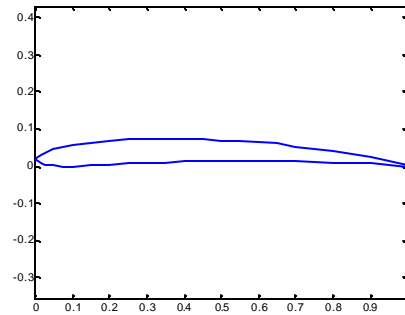


Figure 7: MA409 Airfoil

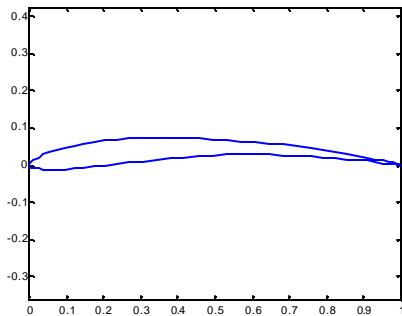


Figure 3: GM15 Airfoil

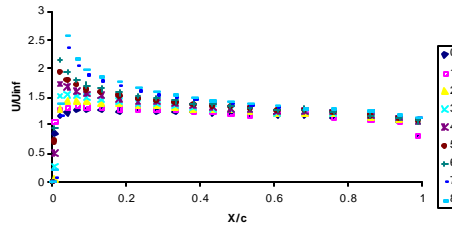


Figure 8: MA409 Velocity Profiles

Figure 4: Velocity Profiles at Positive Angles of Attack

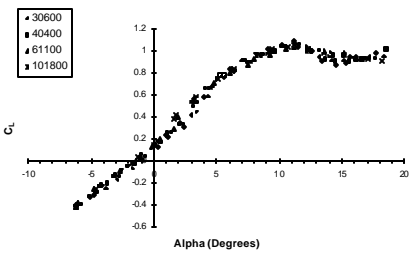
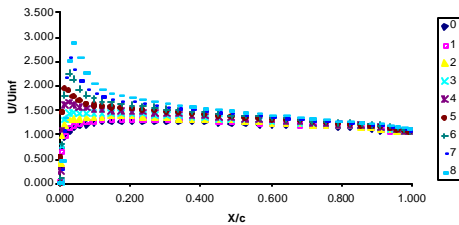


Figure 5: MA409 Lift Curve

The lift and drag curves are direct plots of the experimental data provided in Selig's database, as are the plots of the airfoils. The velocity profiles were both generated using the vortex panel method on the airfoil profiles, some of which were altered slightly to close the trailing edge, as required by the panel method.

Each of these two airfoils performed within requirements over the whole range of expected Reynolds numbers on the blades. Which airfoil will be positioned where was run through an optimization study, and will be explained further in a later section.

## V. Definition of Rotor:

The first step in modeling is to set up the basic geometry of the rotor. Part of the definition of the problem was that it fit inside the already available Mars lander aero-shells to deploy the latest mars rover missions, with only one fold in the blades. The Pathfinder aero-shell has a diameter of  $2.65 \text{ m}^2$ . With one fold in each blade, laying the blades flat, that allows for a total diameter of  $7.95 \text{ m}$ . Allowing some angle in the folded blades means that the radius value can be simplified to  $8 \text{ m}$  for the sake of calculation. As mentioned above, the chord length of the blades must be increased. To this end, they

were defined initially as 0.5 m The following table summarizes the geometry parameters.

#### Blade Parameters

Length	4 m
Width	0.5 m
Disc Area	50.265 m <sup>2</sup>

**Table 3: Rotor Geometry Summary**

Now that the geometry been clearly defined, the rotor needs to be modeled with some basic performance requirements. The simplest model, which justifies continuation of the investigation, is an actuator disc model of the rotor. This treats the rotor as an infinitely thin disc that induces a velocity on the air flowing through it. The induced velocity is used to calculate the power required to lift the aircraft.

The calculation of the induced velocity in an actuator disc model comes from equation 7.

$$v_c = -1/2V_c + \sqrt{1/4V_c^2 + (T/2Ar)} \quad (7)$$

$v_c$  is the induced velocity in climb, and  $V_c$  is the climb rate.  $T$ ,  $A$  and  $\rho$  are the thrust, disc area and density, respectively. In hover,  $V_c = 0$ , and this equation reduces to:

$$v_h = \sqrt{T/2Ar} \quad (7a)$$

The momentum theory that makes use of the actuator disc assumes quasi steady state, even in climb, so thrust equals weight of the aircraft, and the increase in power and induced velocity for climb comes into the math separately.<sup>6</sup>

The induced power requirement, calculated in horsepower, comes from equation 8:

$$HP_c = T(V_c + v_c) / 735 \quad (8)$$

In hover, this reduces to:

$$HP_h = T v_h / 735 \quad (8a)$$

One other important parameter is the rotor tip speed, which is calculated as follows:<sup>7</sup>

$$V_{tip} = \sqrt{\frac{T}{\rho C_T A}} \quad (9)$$

In equation 9,  $C_T$  is the thrust coefficient, which for the moment is assumed 0.03, a typical value.<sup>8</sup>

Table 4 summarizes the results of this preliminary analysis:

Thrust	372.78	N
Rotor Area	50.265	m <sup>2</sup>
Density	0.01503	kg/m <sup>3</sup>
$C_T$	0.03	
Tip Speed	128.24	m/s
Hover		

$v_h$	15.7	m/s
Power	7.97	HP
Climb		
$v_c$	14.3	m/s
Power	8.76	HP
Climb Rate	3	m/s

**Table 4: Actuator Disc Model Summary**

This model gives a slightly lower tip speed than expected, which is a good sign for the continued viability of the project. The next step is to calculate the actual  $C_T$  of the rotor using blade element theory, and use that in the momentum theory, in place of the actuator disc.

The fundamental difference between the actuator disc and the blade element theory is the calculation of induced velocity. In axial flight, (ie hover or climb/descent), the blade is treated as a series of annuli, each inducing a ring of velocity and each drawing a certain amount of power based on the airfoil parameters. The model assumes uniform inflow to the top of the rotor.

This model introduces several new parameters. The first is the lift curve slope of the airfoil section,  $a$ .  $\theta$  is the blade pitch angle, which in axial translation is also the angle of attack of the section. Another new parameter is solidity. Solidity is essentially a ratio of the actual blade area to the total swept disc area, and is calculated by equation 10.

$$s = \frac{Bc}{\rho R} \quad (10)$$

In equation 10,  $B$  is the number of blades,  $c$  is the chord length of the blades, and  $R$  is the radius. Equations 11 and 12 are the integral methods for combining the blade elements to obtain the power required and thrust coefficients in hover. Equation 13 and 14 show the conversion from  $C_T$  to thrust and  $C_P$  to power required.

$$T = C_T \rho A (\Omega R)^2 \quad (11)$$

$$P = C_P \rho A (\Omega R)^3 \quad (12)$$

$$C_T = \int_0^L \frac{s}{2} C_l r^2 dr \quad (13)$$

$$C_P = \frac{k C_T^{3/2}}{\sqrt{2}} + \frac{1}{2} \int_0^L s r^3 C_d dr \quad (14)$$

Above,  $L$  is a tip loss factor, which accounts for the loss due to standard aerodynamic losses at the tips of the rotor blades. From experimental investigation,  $L$  is typically taken as 0.97.  $R$  is the blade radius, and  $\Omega$  is the blade rotation speed in rad/s. In equation 14, the total power is the induced power, based on the  $C_T$ , plus the profile power, the integral. The drag isn't reduced by tip losses, so the drag is integrated out to the tip. Also in

equation 14, the induced power term has an experimental coefficient, because traditional momentum theory under-predicts power by about 10-20%. As such, the constant  $\gamma$  is given a value of 1.15.<sup>9</sup>

From these equations, one of the major trade-off parameters is solidity. In axial flight, solidity is directly proportional to  $C_T$ . However, the parasite power is also directly proportional to solidity, and the induced power requirement is proportional to  $C_T^{3/2}$ , and therefore  $s^{3/2}$ . There is a minimum solidity which must be used to get sufficient thrust, but in general the less solid a blade, the better.<sup>8</sup>

In climb, the inflow velocity must be used, which is a function of the climb rate. This again treats the system in quasi steady state, plus a lifting parameter. It is calculated through the following equations, assuming uniform inflow:

$$v_h = I_h V_{tip} = \frac{P_{id}}{C_T} V_{tip} \quad (15)$$

where  $P_{id}$  is the induced power requirement from the thrust generation, the first term in equation 12. The induced velocity in climb is given by:

$$v = v_h - V_c / 2 \quad (16)$$

where  $V_c$  is the climb rate. The power required for climb is then given by:

$$P_c = T(V + v) \quad (17)$$

and the  $C_p$  is finally given by:

$$C_p = \frac{P_c}{rAV_T^3} \quad (18)$$

## VI. Results for Single Rotor Case

To calculate the blade properties, the individual rotor is broken up into a series of discrete elements, using the non-dimensional radius  $r/R$ . In this case, the rotor was broken up into 17 individual segments, with the elemental length  $dr = 0.0625$ . Then an 18<sup>th</sup> section was defined as  $r/R=B, 0.97-1$ .

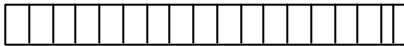


Figure 9: Schematic of blade element definitions <sup>π</sup>

The rotor was designed based on an allowable increase in velocity over the airfoil section chosen. Originally, both the MA409 and GM15 airfoils were intended for use, but during the speed change analyses, it was found the GM15 outperformed the MA409 at all stations, so the wing has a single airfoil shape. This greatly simplifies the

design, making it more attractive in manufacturing terms.

First, the local rotor speed was determined as a fraction of the tip speed. The maximum allowable local speed was set at 230m/s. This, divided by the local rotor speed, was the maximum allowable  $U/U_{inf}$  value over the airfoil surface. This, in turn, led to the local allowable angle of attack based on the velocity profiles. Far enough inboard of the tips, the allowable angle grew to well beyond the maximum angle the wing could handle. At that point, the angle was leveled out at 7 degrees. This is roughly halfway to the maximum lift angle of attack, which occurs between 12 and 15 degrees, depending on the Reynolds number. As seen in figure 2, at the lower Reynolds numbers inboard, this is almost exactly half the maximum angle of attack. This angle avoids hysteresis and stall, and still allows a pitch-up of 3 degrees safely, either collectively or cyclically as flight conditions require.

The solidity was used as an optimization factor to bring the  $C_T$  as close as possible to the 0.03 used in the actuator disc model. This kept the tip speed at the original design condition. The number of blades was used as a gross tuning factor, then the chord length was adjusted down from the initial guess to bring the  $C_T$  in line with the intended value. Table five shows the final configuration of the rotor, and table 6 summarizes the results:

r/R	Chord [m]	Cl	$\gamma$
0	0.43	1.084	7
0.0625	0.43	1.084	7
0.125	0.43	1.084	7
0.1875	0.43	1.084	7
0.25	0.43	1.084	7
0.3125	0.43	1.084	7
0.375	0.43	1.17	7
0.4375	0.43	1.17	7
0.5	0.43	1.17	7
0.5625	0.43	1.14	7
0.625	0.43	1.14	7
0.6875	0.43	1.14	7
0.75	0.43	1.14	7
0.8125	0.43	1.045	7
0.875	0.43	1.045	7
0.9375	0.43	1.077	6
0.97	0.43	1.033	5
1	0.43	0.091	4

Table 5: Blade Geometry

<b>Hover</b>		
$C_T$	0.030678	
Thrust	381.206	N
$C_P$	0.004773	
Power	9.56509	HP
Tip Speed	126.8235	m/s
<b>Climb</b>		
Climb speed	3	m/s
$C_P$	0.005144	
Power	10.30867	HP
<b>Blade Dimensions</b>		
Number of Blades	5	
Blade width	0.43	m
Solidity	0.171	

**Table 5: Single Rotor Blade Element Results**

As can be seen, the required power with the blade element theory is significantly higher, by about 18% in climb and 20% in hover. This model, as applied, is accurate within ~5% of the actual values.

### VII. Alternate Design Concepts

The first computation is for a single rotor, which would require some form of anti-torque device. The tail fan, or other anti-torque would require even more power that contributes nothing meaningful in terms of lift. In this environment, “wasted” power is unacceptable, and the inclusion of the requisite tail boom to support an anti-torque propeller or fan makes fitting the launch capsule difficult. If some form of air-breathing propulsion were used, a NOTAR (NO Tail Rotor) system could be implemented with the exhaust, partially solving the tail-boom problem, but air-breathing systems on Mars may or may not be viable.

The most elegant and simplest solution to implement is the use of counter-rotating rotor blades. In this design, 2 rotors, which spin in opposite directions (i.e. one clockwise, one counterclockwise), provide the anti-torque. The most prevalent example of this is the tandem rotor configuration, fig 9.

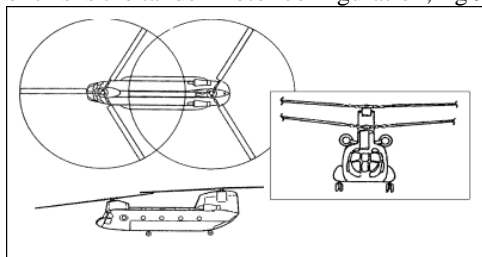


Figure 10: CH47-B Tandem Rotor Helicopter <sup>10</sup>

This design suffers from the same problem as a tail boom, without very, complicated folding mechanisms, it simply will not fit in the lander. Other tandem rotor configurations have the rotors side by side, instead of back to front, but this does not solve the central problem.

The best alternative is a co-axial rotor. This design offers the benefits of automatic counter torque, with the added benefit of decreasing the rotor footprint for the same total thrust.

### VIII. Analysis of Co-Axial Configuration



Figure 11: Ka-25 with Co-Axial Rotors<sup>11</sup>

A Co-axial rotor essentially acts like two independent rotors, with one functioning in a constant climb mode with the induced velocity from the first rotor. However, the slip stream contracts with distance from the rotor plane, as illustrated in fig 12.

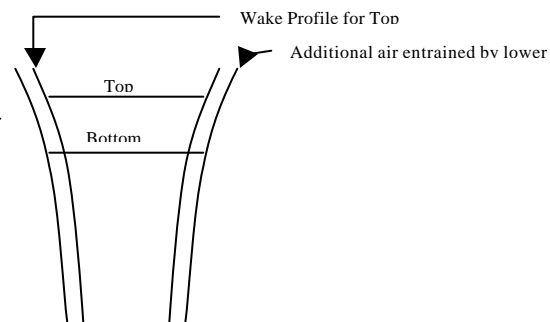


Figure 12: Contraction of rotor wake stream for co-axial helicopters

In hover, the ratio between the width of the fully developed wake and the rotor disc is ~0.707. The wake does not develop fully by the second rotor, but there is a slight effective area bonus on the second rotor which is nearly impossible to calculate without some measurements of the wake field. This area bonus offsets the penalty for having the lower rotor operating with a constant inflow, allowing co-axial rotors to have the same thrust characteristics as 2 independent rotors each producing  $\frac{1}{2}$  the total thrust. <sup>6</sup>

Same Mass	
2 x 0.5T	372 N
Area	25.132 m <sup>2</sup>
Diameter	5.656 m
C <sub>P</sub>	0.009546
P <sub>hover</sub>	9.565 HP
Same Area	
2 x 1 T	745.56 N
Liftable Mass	200kg
C <sub>P</sub>	0.009546
P <sub>hover</sub>	19.78 HP
Same Area, Same Mass	
C <sub>T</sub>	0.015339
C <sub>P</sub>	0.001948
P <sub>hover</sub>	7.809 HP

**Table 6: Co-Axial Lifting Capabilities**

Since the rotor was defined with the dimensionless thrust and power coefficients, it is easy to scale these and determine the power requirements for a co-axial rotor lifting the same mass, as well as seeing how much two of the original rotors could lift.

The obvious benefit with a co-axial configuration is that for the same rotor footprint, one

can lift twice the mass as with a single rotor, though the requisite power is also doubled. Or, conversely, one could lift the same mass with half the rotor footprint. Essentially, a co-axial rotor has the same effect as doubling the disc loading on a single rotor, but with the added benefit of dealing with counter-torque issues simultaneously. The biggest benefit here, though, is using two of the same rotor, to lift the same mass, drastically reduces the required power input because the C<sub>T</sub> is cut in half. This is an attractive option, as electric motors get very heavy as horsepower increases. Being able to shave off even 1 HP from the required power can significantly reduce the mass of the power plant.

### IX. Conclusions

A single rotor to lift 100kg on Mars, at a diameter of 8m, requires a 10.5HP power plant to attain a vertical climb rate of 3 meters per second. A co-axial rotor configuration has significant advantages over a single rotor. For the same overall rotor footprint, a co-axial rotor can either lift twice the required mass in hover for just over twice the required power or the design mass for half the required power. A coaxial rotor lifting the design mass would easily be able to perform the mapping and scouting missions that the helicopter is desired for.

<sup>1</sup> Sermeus, K. "Application of Steady Perfect Gas CFD on Unstructured Grids" Euroavia / Mission to Mars Symposium November, 2002

<sup>2</sup> Bertin, J. "Aerodynamics for Engineers" Fourth Edition. © 2002, Prentice Hall, New Jersey, ISBN: 0-12-064633-4

<sup>3</sup> Halterman, A., Louge, M. "Mars Unmanned Aircraft 2003-2004: Odysseus Team." Cornell University, 2004

<sup>4</sup> Marchman, J. F., Sumantran, V. Schaefer, C.G. "Acoustic and Turbulence Influences on Stall Hysteresis" AIAA-86-0170 January, 1986

<sup>5</sup> Selig, M. "UIUC Airfoil Data Site," Department of Aerospace Engineering University of Illinois at Urbana-Champaign, Urbana, Illinois 61801 Available: <http://www.aae.uiuc.edu/m-selig/ads.html>

<sup>6</sup> Stepniewski, W.Z., Keys, C.N., "Rotary Wing Aerodynamics" © 1984, Dover Publications New York, ISBN: 0-486-64647-5

<sup>7</sup> McCormick, Barnes, "Aerodynamics of V/STOL Flight," © 1999, Dover Publishing, New York ISBN: 0-486-40460-9

<sup>8</sup> Etchells, David "The Design and Development of a Mars Airborne Exploratory Vehicle." Aeronautical Engineering Masters Thesis, Loughborough University, Summer 2003

<sup>9</sup> Johnson, Wayne. "Helicopter Theory," © 1980, Dover Publications, New York, ISBN: 0-486-68230-7

<sup>10</sup> Global Security.org, "Army Field Manuals." © 2000-2004 GlobalSecurity.org Available: <http://www.globalsecurity.org/military/library/policy/army/fm/3-21-38/appb.htm>

<sup>11</sup> Centennial of Flight, "Helicopter Rotor Configurations," © 2003, available: [http://www.centennialofflight.gov/essay/Dictionary/heli\\_rotor\\_config/DI54.htm](http://www.centennialofflight.gov/essay/Dictionary/heli_rotor_config/DI54.htm)